Ordering of localized electronic states in multiferroic TbMnO$_3$: a soft x-ray resonant scattering study

FAST TRACK COMMUNICATION

Ordering of localized electronic states in multiferroic TbMnO₃: a soft x-ray resonant scattering study

T R Forrest[1], S R Bland[2], S B Wilkins[3], H C Walker[1], T A W Beale[2], P D Hatton[2], D Prabhakaran[4], A T Boothroyd[4], D Mannix[5], F Yakhou[6] and D F McMorrow[1]

[1] London Centre for Nanotechnology, University College London, Gower Street, London WC1E 6BT, UK
[2] Department of Physics, University of Durham, Rochester Building, South Road, Durham DH1 3LE, UK
[3] Brookhaven National Laboratory, Condensed Matter Physics and Material Science Department, Building #501B, Upton, NY 11973-5000, USA
[4] Department of Physics, University of Oxford, Clarendon Laboratory, Parks Road, Oxford OX1 3PU, UK
[5] Institut Néel, CNRS-UJF, BP166, 38042 Grenoble, France
[6] European Synchrotron Radiation Facility, BP220, 38043 Grenoble, France

E-mail: t.forrest@ucl.ac.uk

Abstract

Soft x-ray resonant scattering (XRS) has been used to observe directly, for the first time, the ordering of localized electronic states on both the Mn and the Tb sites in multiferroic TbMnO₃. Large resonant enhancements of the x-ray scattering cross-section were observed when the incident photon energy was tuned to either the Mn L or Tb M edges which provide information on the Mn 3d and Tb 4f electronic states, respectively. The temperature dependence of the XRS signal establishes, in a model independent way, that in the high-temperature phase (28 K $\leqslant T \leqslant$ 42 K) the Mn 3d sublattice displays long-range order. The Tb 4f sublattices are found to order only on entering the combined ferroelectric/magnetic state below 28 K. Our results are discussed with respect to recent hard XRS experiments (sensitive to spatially extended orbitals) and neutron scattering.

(Some figures in this article are in colour only in the electronic version)

1. Introduction

Magnetoelectric multiferroics are materials that simultaneously display ferroelectric and magnetic long-range order [1]. Consequently, they are of considerable interest both from a fundamental point of view, and for the potential that they offer in the field of spintronics [2, 3]. Of particular importance has been the recent discovery of multiferroic behavior in a diverse range of compounds where the multiferroic state takes the form of the coexistence of ferroelectricity and antiferromagnetism, often with a large coupling between the two [4, 5]. Indeed the burgeoning interest in multiferroics can be traced to the pioneering work by Kimura *et al* who demonstrated a giant magnetoelectric effect in TbMnO₃ where the electric polarization may be switched by applying a magnetic field [6]. More recently it has been shown how an applied electric field can be used to manipulate the magnetic domain distribution [7].

For TbMnO₃ (space group *Pbmn*) the Mn³⁺ magnetic moments first order below $T_{N1} = 42$ K. It has been reported,

based on recent neutron diffraction data, that below this
temperature the moments are polarized along the **b** direction
with a modulation wavevector (0 q_{Mn} 0), $q_{Mn} \approx 0.29\,b^*$.
Below $T_{N2} = 28$ K the magnetic structure adopted by the Mn
sublattice becomes non-collinear, forming a cycloid in the **b**–**c**
plane [8] and, at exactly the same temperature, a ferroelectric
polarization along the **c** direction is observed. By comparing
the magnetic structures above and below T_{N2}, an elegant
and appealing model was proposed whereby the ferroelectric
transition is driven by a loss of inversion symmetry at the Mn
sites as the magnetic structure changes from collinear to non-
collinear. The same study also proposed that the Tb magnetic
moments are disordered in the collinear phase, and become
polarized along the **a** direction on cooling into the cycloidal
phase.

X-ray resonant scattering (XRS) has much to offer the
study of multiferroics in general [9–12], and TbMnO₃ in
particular. It is an element and electron shell specific technique,
which in the case of TbMnO₃ makes it possible to study any
ordering of the Mn and Tb sublattices separately. Neutron
diffraction by contrast measures the scattering from the sum
of the separate contributions. Moreover, XRS is capable
of providing information on the presence of any multipolar
order [13]. This includes multipoles with time-odd, parity-
odd symmetry that may characterize the combined magnetic
and ferroelectric state displayed by TbMnO₃ and other related
multiferroics [14]. Recently the results of a number of XRS
studies of TbMnO₃ have been reported, all performed in the
hard part of the x-ray spectrum above 3 keV [15, 16]. The
edges accessed in this part of the spectrum are the Mn K and
Tb L₃ edges which, for the dominant electric dipole resonances
observed, provide information on the ordering of the 4p and 5d
extended band states at the Mn and Tb sites, respectively. Here
we highlight two of the main results of this x-ray work [15].
The first is the surprising observation of a large polarization
of the Tb 5d states in the collinear phase, where according to
modeling of the neutron data the Tb magnetic moments are
disordered. The second is the tentative report that the 5d states
develop an anapolar moment, i.e. one with time-odd, parity-
odd symmetry, in the cycloidal phase.

In order to shed further light on the ordering of the
different electronic states in TbMnO₃ we have utilized XRS
in the vicinity of the Mn L₂ (649.9 eV: $2p_{3/2} \rightarrow 3d$) and L₃
(638.7 eV: $2p_{5/2} \rightarrow 3d$) and the Tb M₄ (1276.9 eV: $3d_{3/2} \rightarrow 4f$) and M₅ (1241.1 eV: $3d_{5/2} \rightarrow 4f$) edges. The clear benefit
of utilizing these edges is that they provide information on the
localized 3d and 4f states. In this sense our soft x-ray study
of TbMnO₃ is complementary to both neutron diffraction and
hard XRS studies. There are, however, limitations as to what
can be achieved with soft x-rays. For example, when compared
to the studies performed with photon energies above 3 keV, the
Ewald sphere of reciprocal space is severely limited.

One complication encountered in any study of TbMnO₃,
in addition to the ordering of both the Tb and Mn sublattices,
is the existence of a complex magnetic domain structure.
Four possible domain states have been identified, which can
be classified according to the Miller indices (h, k, l) of the
associated satellite peaks: A ($h + k =$ even, $l =$ odd), C

($h + k =$ odd, $l =$ even), F ($h + k =$ even, $l =$ even), and G
($h + k =$ odd, $l =$ odd). The relative population of domains
is found to differ from study to study [17–19, 8], although the
A domain dominates in most cases reported. In our soft XRS
study, the limited range of reciprocal space available had the
consequence that only F-type satellite reflections fall within the
Ewald sphere at the Mn L edges, while at the Tb M edges A, C
and F satellites can in principle be accessed.

2. Experimental details

Single crystals of TbMnO₃ with dimensions $2 \times 2 \times 1$ mm³
were grown at the University of Oxford using the flux growth
method. They were cut with either the [0 1 0] or [0 0.28 1]
directions as the surface normal and polished with 0.1 μm
diamond followed by 0.02μ Al₂O₃ pastes, to a flat, shiny
surface. Experiments were carried out on both beamline 5U1
at the SRS, Daresbury Laboratory and ID08 at the European
Synchrotron Radiation Facility. The former beamline was used
to collect the temperature dependence of the scattering, while
the latter was used for its superior flux and high incident photon
energy resolution to determine the energy dependence of the
scattering. These measurements were conducted in a similar
fashion to that of Wilkins *et al* [20–22] on both beamlines. The
samples were mounted on the diffractometer with the surface
normal and [001] direction lying within the scattering plane.
In both cases, the diffraction plane was vertical. At 5U1 and
ID08 the base temperatures achievable were 22 K and 19 K
respectively. Due to experimental apparatus limitations it was
not possible to measure the polarization of the scattered x-rays.

3. Results and discussion

We first consider the results for the Mn L edges taken using the
[0 1 0] oriented sample. On cooling below $T_{N1} \approx 42$ K an
F-type satellite diffraction peak was observed at (0 q 0), with
$q \approx 0.295\,b^*$ just below T_{N1}. The peak was present at both
the L₂ and L₃ edges, and was found to increase in intensity and
move to lower q as the temperature was decreased (figures 1(a)
and (b) peak). By fitting this satellite peak to a Lorentzian
line shape, the correlation lengths (defined as $\zeta = \frac{1}{\kappa}$, where
κ is the characteristic half width of the Lorentzian distribution
in reciprocal lattice units) were determined to exceed 200 Å
at both the L₂ and L₃ edges, and in both the cycloidal and
collinear phases. This result demonstrates that the x-rays probe
a significant number of unit cells within the crystal and hence,
these measurements are not particularly surface sensitive.

A scan of the incident photon energy at fixed wavevector
transfer in the high-temperature collinear phase revealed strong
enhancements of the scattering cross-section at the Mn L₂
and L₃ edges (figure 1(c)). While a simple, single resonant
response is evident at the L₂ edge, the energy line shape
displays much more structure in the vicinity of the L₃ edge.
Notwithstanding these important details, the strong electric
dipole resonances, combined with the sharpness of the peaks in
reciprocal space, establishes the fact that the Mn 3d electronic
states display long-range order in the collinear phase. In
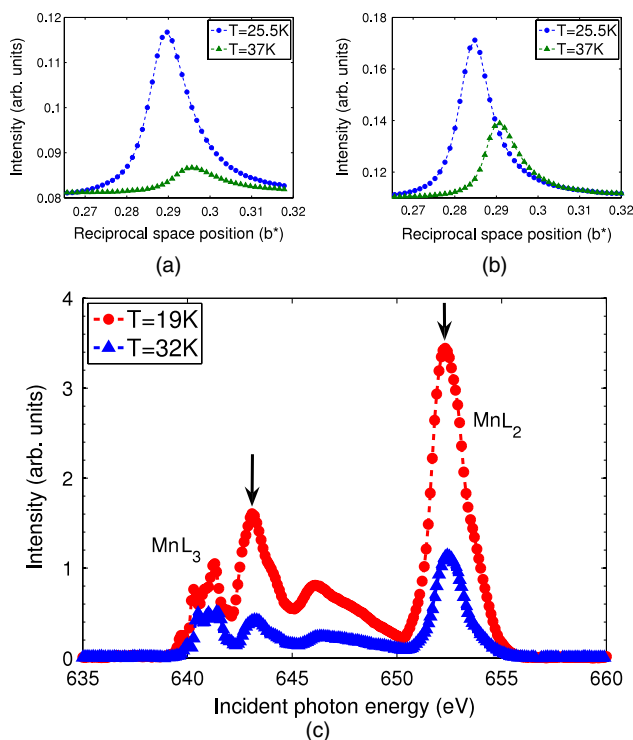figure 1(c) the results of an energy scan in the cycloidal phase

Figure 1. θ–2θ scan of the (0 q 0) reflection in the cycloidal (25.5 K) and collinear (32 K) phases collected with incident x-ray photon energies equal to (a) the Mn L_3 resonance (639 eV) and (b) the Mn L_2 resonance (652 eV) as determined from (c) an energy scan at fixed wavevector of the (0 q 0) reflection in the two phases. The vertical arrows indicate the energies at which a temperature dependence was recorded.

Figure 2. Temperature dependence of the (0 q 0) superlattice reflection: (a) the position and (b) the integrated intensity at the Mn L_2 (652.3 eV) and L_3 (643.1 eV) edges. (c) the integrated intensity of the (0 q 1) superlattice reflection at the Tb M_5 edge (1240 eV), (an offset of -2 K has been applied to this data). Finally (d) is the integrated intensity of the (0 1 $- q$ 0) superlattice reflection, again this was recorded with photons equal in energy to the Tb M_5 edge (1240 eV).

at 19 K are also shown. Apart from an overall increase in intensity, the response in this phase is indistinguishable from that in the collinear one.

It should be noted that a number of soft x-ray resonant scattering studies have been made of related rare-earth manganite compounds, which are not multiferroic [20–23]. Results from all of these studies have shown that, for both the magnetic and orbital reflections, the resonant feature at the Mn L_3 edge is always strongest. This is clearly not the case for the (0 q 0) reflection observed in this study. However, to obtain further information from this fixed wavevector energy scan, detailed modeling of the electronic structure is required, which is beyond the scope of the present work.

Scans parallel to **b***, across the (0 q 0) reflection were performed as a function of temperature at incident photon energies equal to the main features of the Mn L_2 and L_3 resonances shown in figure 1(c). Figure 2 shows the temperature dependence of (a) the position and (b) the integrated intensity of the peak obtained by fitting a Lorentzian function to the peak profiles. In the cycloidal/ferroelectric phase below 28 K, the propagation vector is only weakly temperature dependent with $q \simeq 0.285b^*$ before increasing linearly with increasing temperature within the collinear phase to a maximum value of $q \simeq 0.295b^*$ at $T = 42$ K. This trend is consistent with that deduced by neutron and hard x-ray scattering experiments [8, 15]. Above 42 K the peak was not observed. The evolution of the integrated
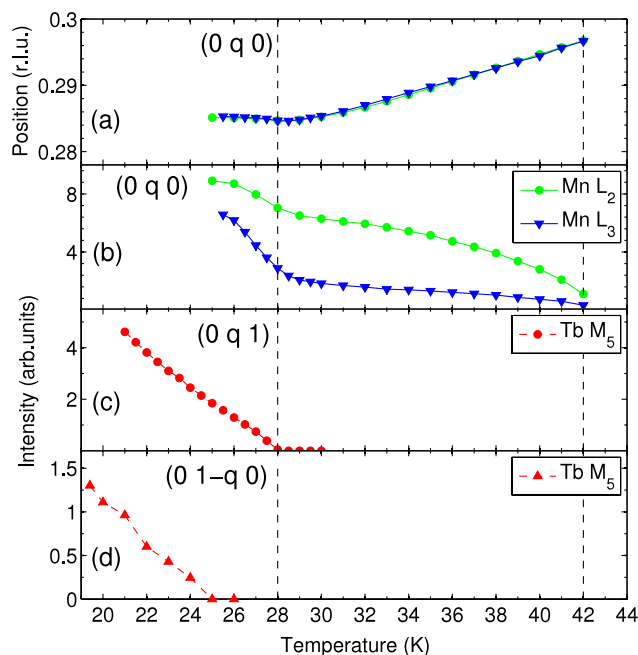
intensity as a function of temperature clearly differs between the measurements performed at the Mn L_2 and L_3 edges, with a more significant change at the L_3 edge at the transition between the two magnetic phases. In other words the L_2/L_3 branching ratio is temperature dependent. A strongly temperature dependent branching ratio has previously been observed in $DyFe_4Al_8$, which was attributed to the effect of magneto-elastic coupling [24].

The fact that the main resonances occur at the Mn L_2 and L_3 edges indicates that the electric dipolar (E1) resonance dominates and therefore the Mn 3d electronic states are being probed. When this is combined with the observation, that the thermal evolution of the wavevector shown in figure 2(a) tracks that of the fundamental magnetic wavevector **q** determined by neutron diffraction, the conclusion that the XRS in this experiment is most probably magnetic in origin may be drawn. The only other possible order parameter that might be probed using XRS for a purely dipolar transition is that associated with ordering of the electric quadrupole (orbital ordering) which these experiments do not exclude.

We now consider the results taken with photon energies close to the Tb M_4 and M_5 edges. In contrast to the Mn L edges, where only the F-type reflection may be observed, at the Tb M edges, A-and C-type reflections are also accessible. (To observe the A-type reflection, the [0 1 0] was replaced by the [0 0.28 1] orientated sample.) Comprehensive searches in the collinear phase for any of these reflections produced negative results. On cooling into the cycloidal phase, strong, well-
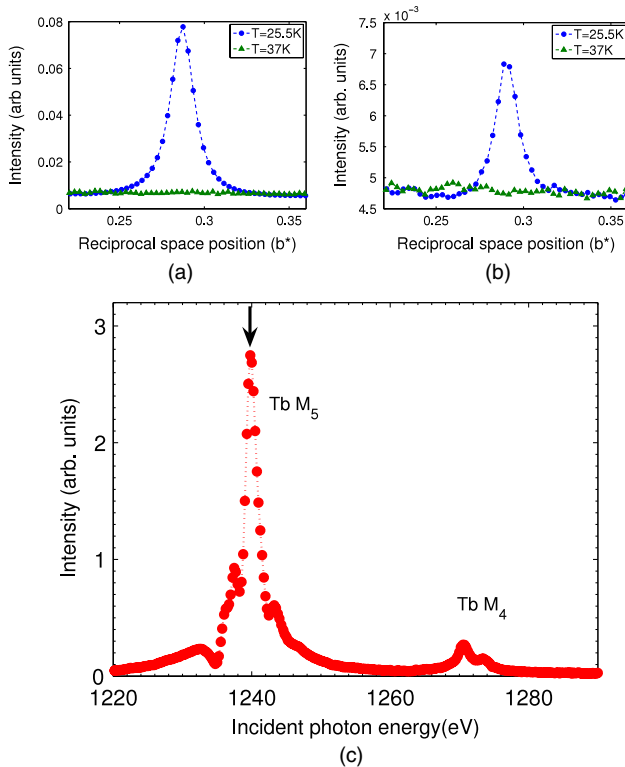
Figure 3. θ–2θ scan of the (0 q 1) reflection in the cycloidal phase at $T = 26$ K collected with incident x-ray photon energies equal to (a) the Tb M_5 resonance (1240 eV) and (b) the Tb M_4 resonance (1271 eV) as determined from (c) an energy scan at fixed wavevector of the (0 q 1) reflection. The vertical arrow indicates the energy at which a temperature dependence was recorded.

defined A-type reflections appeared at both the M_4 and M_5 edges. The sharpness of the diffraction profiles (figures 3(b) and (a)) immediately establishes that the electronic states (in this case the Tb 4f states) are long-range ordered. Figure 3(c) shows a energy scan at the fixed wavevector of the (0 q 1) reflection in the cycloidal phase, demonstrating significant resonances at the M_5 edge and M_4 edges. This indicates that for the (0 q 1) reflection, the Tb 4f electronic states are strongly influenced by the cycloidal magnetic order. Figure 2(c) shows the temperature dependence of the scattered intensity of the A-type (0 q 1) reflection taken at the Tb M_5 edge. As for the F-type peak, where the results were taken at the Mn L edges, the magnitude of the modulation wavevector evolves as a function of temperature. For this crystal orientation, however, the reflection becomes off-specular. Experimental limitations at 5U1 made it impossible to accurately resolve the evolution of peak's position as the temperature was increased, and hence here we only present the integrated intensity as a function of temperature, determined as for the (0 q 0) reflection. As can be seen, the intensity of the scattering at the M_5 edge drops rapidly and linearly with increasing temperature, with zero intensity being observed for $T \geqslant 30$ K. Hence, it would appear that in this domain the localized Tb 4f states are strongly affected by the cycloidal order, but not by the collinear magnetism.

For the F-type (0 q 0) reflection, a very weak resonance was observed in the cycloidal phase at the Tb M_5-edge, but

only with π-polarized incident photons. However, a stronger Tb M_5 resonance reflection was observed at a position of (0 $\sim$0.78b^* 0). This superlattice reflection corresponds to the C-type (0 1 − q 0) domain. Like the F-type reflection, the peak was only observed with π-polarized incident photons. Figure 2(d) shows the temperature dependence of the scattered intensity for this (0 1 − q 0) peak. As the temperature was increased, the intensity of the scattering at the Tb M_5 edge decreased, with zero intensity being observed for $T \geqslant 24$ K. The position of this peak remained constant as the temperature was increased.

Finally, we note that fixed wavevector energy scans for the F-type (0 q 0) reflection failed to identify any clear response in the vicinity of the oxygen K (543.1 eV: 1s → 2p) edge.

4. Conclusions

In conclusion, we have performed the first direct element specific study of the effect of the magnetic order on the electronic structure of magnetoelectric multiferroic $TbMnO_3$. We have demonstrated that the Mn 3d localized bands display strong long-range order in both magnetic phases for the F-type domain. The temperature dependence of this (0 q 0) reflection is in good agreement with previously observed trends for both the position of the modulation wavevector (0 q_{Mn} 0) and the scattered intensity, with clear changes at the magnetic phase transitions. Mn L edge energy scans at this wavevector show minimal changes in the overall 3d band structure between the collinear and cycloidal phases. The scattered intensity as a function of temperature does differ, however, between measurements performed at the Mn L_2 and L_3 edges. The transition at 28 K into the ferroelectric phase is more significant for the measurements performed at the Mn L_3 edge. The energy scans taken at the Tb M edges clearly show, that for the A-type (0 q 1) reflection, the Tb 4f band is highly influenced by the cycloidal magnetic order, whilst this reflection was absent in the collinear phase, indicating that there is no long-range ordering of the Tb 4f states for this phase. This data supports the neutron diffraction model which states that the Tb 4f states should be disordered in the collinear phase. However the absence of Tb 4f ordering in the collinear phase suggests that ordering of Tb 5d bands as seen with hard x-rays [15] is of a different origin. In addition to strong Tb M edge resonances observed for the A-type peak, much weaker Tb M edge resonance peaks corresponding to the F-type (0 q 0) and C-type (0 1 − q 0) reflections were observed in the cycloidal phase. The fact that these two reflections were observed with π-incident x-rays only and are much weaker, suggest a difference between the magnetic structures of the domain states. Finally, the lack of an F-type reflection in the vicinity of the oxygen K edge, shows that for this reflection at least, there is no long-range ordering of the oxygen 2p band.

References

[1] Eerenstein W, Mathur N D and Scott J F 2006 *Nature* **442** 759
[2] Fiebig M 2005 *J. Phys. D: Appl. Phys.* **38** R123–52
[3] Spaldin N A and Fiebig M 2005 *Science* **309** 391–2
[4] Hill N A 2000 *J. Phys. Chem.* B **104** 6694
[5] Cheong S-W and Mostovoy M 2007 *Nat. Mater.* **6** 13
[6] Kimura T, Goto T, Shintani H, Ishizaka K, Arima T and Tokura Y 2003 *Nature* **426** 55
[7] Yamasaki Y, Sagayama H, Goto T, Matsuura M, Hirota K, Arima T and Tokura Y 2007 *Phys. Rev. Lett.* **98** 147204
[8] Kenzelmann M, Harris A B, Jonas S, Broholm C, Schefer J, Kim S B, Zhang C L, Cheong S-W, Vajk O P and Lynn J W 2005 *Phys. Rev. Lett.* **95** 087206
[9] Ewings R A, Boothroyd A T, McMorrow D F, Mannix D, Walker H C and Wanklyn B M R 2008 *Phys. Rev.* B **77** 104415
[10] Prokhnenko O, Feyerherm R, Dudzik E, Landsgesell S, Aliouane N, Chapon L C and Argyriou D N 2007 *Phys. Rev. Lett.* **98** 057206
[11] Yang C-H, Koo J, Song C, Koo T Y, Lee K-B and Jeong Y H 2006 *Phys. Rev.* B **73** 224112
[12] Koo J, Song C, Ji S, Lee J-S, Park J, Jang T-H, Yang C-H, Park J-H, Jeong Y H, Lee K-B, Koo T Y, Park Y J, Kim J-Y, Wermeille D, Goldman A I, Srajer G, Park S and Cheong S-W 2007 *Phys. Rev. Lett.* **99** 197601
[13] Di Matteo S, Joly Y and Natoli C R 2005 *Phys. Rev.* B **72** 144406
[14] Van Aken B, Rivera J-P, Schmid H and Fiebig M 2008 *Nature* **449** 702
[15] Mannix D, McMorrow D F, Ewings R A, Boothroyd A T, Prabhakaran D, Joly Y, Janousova B, Mazzoli C, Paolasini L and Wilkins S B 2007 *Phys. Rev.* B **76** 184420
[16] Argyriou D N, Aliouane N, Strempfer J, Zegkinoglou I, Bohnenbuck B, Habicht K and Zimmermann M v 2007 *Phys. Rev.* B **75** 020101
[17] Quezel S, Tcheou F, Rossatmignod J, Quezel G and Roudaut E 1977 *Physica* B + C **86** 916
[18] Blasco J, Ritter C, García J, de Teresa J M, Pérez-Cacho J and Ibarra M R 2000 *Phys. Rev.* B **62** 5609–18
[19] Kajimoto R, Yoshizawa H, Shintani H, Kimura T and Tokura Y 2004 *Phys. Rev.* B **70** 012401
[20] Wilkins S B, Spencer P D, Hatton P D, Collins S P, Roper M D, Prabhakaran D and Boothroyd A T 2003 *Phys. Rev. Lett.* **91** 167205
[21] Wilkins S B, Hatton P D, Roper M D, Prabhakaran D and Boothroyd A T 2003 *Phys. Rev. Lett.* **90** 187201
[22] Wilkins S B, Stojic N, Beale T A W, Binggeli N, Castleton C W M, Bencok P, Prabhakaran D, Boothroyd A T, Hatton P D and Altarelli M 2005 *Phys. Rev.* B **71** 245102
[23] Thomas K J, Hill J P, Grenier S, Kim Y-J, Abbamonte P, Venema L, Rusydi A, Tomioka Y, Tokura Y, McMorrow D F, Sawatzky G and van Veenendaal M 2004 *Phys. Rev. Lett.* **92** 237204
[24] Langridge S, Paixao J A, Bernhoeft N, Vettier C, Lander G H, Gibbs D, Sorensen S A, Stunault A, Wermeille D and Talik E 1999 *Phys. Rev. Lett.* **82** 2187–90